Breathers in Two-Dimensional Neural Media

S. E. Folias[1] and P. C. Bressloff[1]
[1]*Department of Mathematics, University of Utah, Salt Lake City, UT 84112*

(Dated: July 25, 2005)

In this Letter we show how nontrivial forms of spatially localized oscillations or *breathers* can occur in two–dimensional excitable neural media with short-range excitation and long–range inhibition. The basic dynamical mechanism involves a Hopf bifurcation of a stationary pulse solution in the presence of a spatially localized input. Such an input could arise from external stimuli or reflect changes in the excitability of local populations of neurons as a precursor for epileptiform activity. The resulting dynamical instability breaks the underlying radial symmetry of the stationary pulse, leading to the formation of a nonradially symmetric breather. The number of breathing lobes is consistent with the order of the dominant unstable Fourier mode associated with perturbations of the stationary pulse boundary

PACS numbers: 87.19.La, 87.10.+e, 05.45.-a

Analysis of the dynamical mechanisms underlying spatially structured activity states in neural tissue is crucially important for understanding a wide range of neurobiological phenomena, both naturally occurring and pathological. For example, neurological disorders such as epilepsy are characterized by spatially localized oscillations and waves propagating across the surface of the brain [1], whilst traveling waves can be induced *in vitro* by electrically stimulating disinhibited cortical slices [2, 3]. Spatially coherent activity states are also prevalent during the normal functioning of the brain, encoding local properties of visual stimuli [4], representing head direction [5], and maintaining persistent activity states in short–term working memory [6]. One of the major challenges in neurobiology is understanding the relationship between spatially structured activity states and the underlying neural circuitry that supports them. This has led to considerable recent interest in studying reduced neural field models [7–10], in which the large–scale dynamics of populations of neurons is described in terms of a nonlinear integrodifferential equation whose associated integral kernel represents the spatial distribution of neuronal synaptic connections. Such models provide an important example of spatially extended excitable systems with nonlocal interactions.

In this Letter we show how nontrivial forms of spatially localized oscillations or *breathers* can occur in neural field models in the presence of spatially localized stationary inputs. Such inputs could arise from external stimuli or reflect changes in the excitability of local populations of neurons as a precursor for epileptiform activity. Previously, we have shown that breathers can arise in a purely excitatory network (with a positive integral kernel) through a Hopf bifurcation of a stationary pulse centered about the input [11, 12]. An analogous mechanism occurs in nonlinear PDE models of diffusively coupled excitable media, which is consistent with the observation that an excitatory neural network can be reduced to an equivalent PDE model for certain choices of the interaction kernel [13]. Here we investigate the occurrence of breathers in a two–dimensional network with excitatory and inhibitory interactions, both of which are present in the intact cortex. We show that nonlocal inhibition leads to a new form of symmetry breaking dynamical instability, whereby a two-dimensional radially symmetric stationary pulse bifurcates to a nonradially symmetric breather with an integral number of lobes. We also establish using linear stability analysis that the number of breathing lobes corresponds to the dominant unstable Fourier mode associated with perturbations of the stationary pulse boundary.

We proceed by considering neural field equations of the form [9]

$$\begin{aligned} \tau \frac{\partial u}{\partial t} &= -u + w * f(u) - \beta \varrho + I \\ \frac{1}{\epsilon}\frac{\partial \varrho}{\partial t} &= -\varrho + u. \end{aligned} \tag{1}$$

where

$$\Big(w * f(u)\Big)(\mathbf{r},t) = \int_{\mathbb{R}^2} w(|\mathbf{r}-\mathbf{r}'|) f(u(\mathbf{r}',t)) d\mathbf{r}'$$

where $\mathbf{r} = (r,\theta)$ and $\mathbf{r}' = (r',\theta')$. The neural field $u(\mathbf{r},t)$ represents the local activity of a population of neurons at position $\mathbf{r}$, while $\varrho(\mathbf{r},t)$ represents a local negative feedback mechanism, such as spike-rate adaptation, with ϵ, β determining the relative rate and strength of feedback. τ is a synaptic or membrane time constant, I is an external input, and f denotes an output firing rate function. The homogeneous weight distribution $w(|\mathbf{r}-\mathbf{r}'|)$ defines the strength of the synaptic connections between neurons at $\mathbf{r}$ and $\mathbf{r}'$. Two common forms of the weight function are *excitatory*, i.e., a positive, monotonically decreasing function, or *Mexican hat*, i.e., short–range excitation (positive) and long–range inhibition (negative), often represented by a difference of Gaussians or exponentials. Let us consider the existence and stability of a radially-symmetric, stationary pulse of Eq. (1) for a homogeneous Mexican hat weight w. We proceed by expanding our previous analysis of excitatory networks [12]. As a simplification we take $f(u) = H(u-\kappa)$ where H denotes the Heaviside function and κ a threshold, and for concreteness we consider radially symmetric Gaussian inputs $I(r) = \mathcal{I}\mathrm{e}^{-r^2/\sigma^2}$. We fix the units of time by setting $\tau = 1$ (typically $\tau = 10$ ms). From symmetry arguments we expect the existence of a radially symmetric, stationary pulse $(u(\mathbf{r},t), \varrho(\mathbf{r},t)) = (U(r), Q(r))$, satisfying $Q = U$, with $U(a) = \kappa$, $\kappa < U(r) < \infty$ for $r \in [0,a)$, $U(r) < \kappa$ for $r \in (a,\infty)$. The profile of the pulse is

$$(1+\beta)U(r) = M(a,r) + I(r)$$

where

$$M(a,r) = \int_0^{2\pi}\int_0^a w(|\mathbf{r}-\mathbf{r}'|)r'dr'd\theta. \tag{2}$$

For a given weight distribution w, we can determine pulse existence curves by imposing the self-consistency (threshold) condition $U(a) = \kappa$, which implies that

$$(1+\beta)\kappa = M(a,a) + I(a), \tag{3}$$

This defines the nonlinear relationship between the input strength $\mathcal{I}$ and the pulse width a. In Fig. 1-b we plot existence curves for the Mexican hat weight function

$$w(r) = \frac{a_e}{{\sigma_e}^2}w_{\mathrm{K}}(r/\sigma_e) - \frac{a_i}{{\sigma_i}^2}w_{\mathrm{K}}(r/\sigma_i) \tag{4}$$

where $w_{\mathrm{K}}(r) = (2/3\pi)[K_0(rs) - K_0(2rs)]$ and K_ν is the modified Bessel function of the second kind; see Fig. 1-a . This choice allows $M(a,r)$ to be expressed as a finite sum of modified Bessel functions, and the coefficient $2/3\pi$ fits $w_{\mathrm{K}}(r)$ to the exponential function $\mathrm{e}^{-r}/(2\pi)$ [12].

Linear stability of the stationary pulse is determined by the evolution of small time-dependent perturbations $u(\mathbf{r},t) = U(r) + \bar{\varphi}(\mathbf{r},t)$ and $\varrho(\mathbf{r},t) = Q(r) + \bar{\psi}(\mathbf{r},t)$ which, to first order in $\bar{\varphi}, \bar{\psi}$, satisfy the linearized system

$$\begin{aligned}\frac{\partial\bar{\varphi}}{\partial t} &= -\bar{\varphi} + w * \left[H'(U-\kappa)\bar{\varphi}\right] - \beta\bar{\psi}\\ \frac{1}{\epsilon}\frac{\partial\bar{\psi}}{\partial t} &= -\bar{\psi} + \bar{\varphi}.\end{aligned} \tag{5}$$

We investigate saddle-node and Hopf bifurcations thereof, by relating the eigenvalues to the gradient of the input I. Taking $\bar{\varphi}(\mathbf{r},t) = \varphi(\mathbf{r})e^{\lambda t}$ and $\bar{\psi}(\mathbf{r},t) = \psi(\mathbf{r})e^{\lambda t}$ and using the identity $H'(U(r)-\kappa) = \delta(r-a)/|U'(a)|$ leads to the spectral problem in λ

$$\mu\,\varphi(\mathbf{r}) = \int_0^{2\pi} w(|\mathbf{r}-\mathbf{a}'|)\varphi(a,\theta')d\theta' \tag{6}$$

where $\mathbf{a}' = (a,\theta')$, and μ relates to λ by

$$\lambda + 1 + \frac{\epsilon\beta}{\lambda+\epsilon} = \frac{\mu}{|U'(a)|}.$$

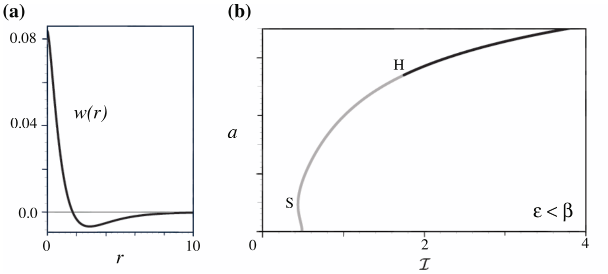

FIG. 1: (a) Plot of the Mexican hat weight function w for $a_e = 1$, $\sigma_e = 1$, $a_i = 1.4$, $\sigma_i = 1.8$. (b) Corresponding pulse existence curves with black (gray) indicating stability (instability) of the stationary pulse solution. S and H indicate saddle-node and Hopf bifurcation points, respectively. Other parameters are $\kappa = 0.15$, $\beta = 2.25$, $\epsilon = 0.03$, $\sigma = 2.4$.

The essential spectrum, associated with the set of functions φ for which the integral in (6) vanishes, is always negative and does not incur instability. Stability thus depends upon the point spectrum, which is associated with functions φ satisfying

$$\mu\,\varphi(a,\theta) = a\int_0^{2\pi} w\big(2a\sin\phi\big)\varphi(a,\theta-\phi)d\phi \tag{7}$$

By requirement of periodicity, solutions of this equation are exponential functions $e^{in\theta}$, where $n \in \mathbb{Z}$, with corresponding *spatial* eigenvalues

$$\mu_n(a) = 2a\int_0^{\pi} w\big(2a\sin\phi\big)\cos(2n\phi)d\phi,$$

which are real and depend on the pulse width a. The eigenvalues associated with the linearization (5) are then

$$\lambda_n^{\pm} = \frac{1}{2}\left(-\Lambda_n \pm \sqrt{\Lambda_n^2 - 4\epsilon(1+\beta)(1-\Gamma_n)}\right), \qquad n \geq 0,$$

where

$$\Lambda_n = 1 + \epsilon - \Gamma_n(1+\beta), \qquad \Gamma_n = \frac{\mu_n(a)}{(1+\beta)\,|U'(a)|}.$$

Stability of the stationary pulse is determined by the gradient of the current input $D(a) = |I'(a)|$ according to

$$\epsilon > \beta: \;\; D(a) > \mu_n(a) - M_r(a) \equiv D_{\mathrm{SN}}(a) \tag{8}$$

$$\epsilon < \beta: \;\; D(a) > \left(\frac{1+\beta}{1+\epsilon}\right)\mu_n(a) - M_r(a) \equiv D_c^n(a) \tag{9}$$

where $M_r(a) = -\partial M(a,r)/\partial r|_{r=a}$. The modified Bessel weight w_{K} allows $M_r(a)$ and $\mu_n(a)$, for all n, to be expressed as finite sums of modified Bessel functions. Points of equality in (8) are associated with saddle-node bifurcations, while that of (9) correspond to Hopf bifurcations of the stationary pulse. Note, conditions (8)-(9) are valid when $M_r(a) > 0$, which is always true for an

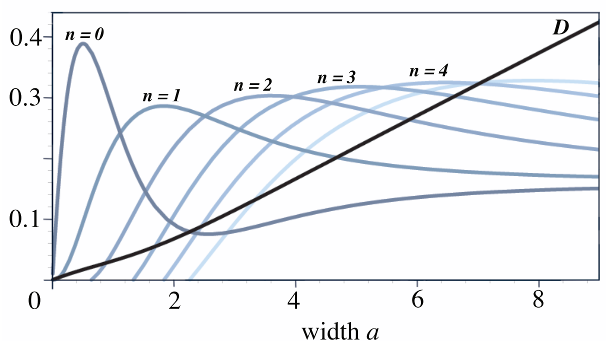

FIG. 2: Plot of the the functions $D(a)$ (black curve) and $D_c^n(a)$ (blue curves) for different values of n with $\sigma = 5.2$; see Fig. 1 for other parameters. The stationary pulse is stable if $D(a) > D_c^n(a)$ for all n, with a Hopf bifurcation occurring at the first value of a for which this is no longer true. The largest $D_c^n(a)$ determines the mode that dominates the instability for pulse width a, e.g., a value of $\mathcal{I} = 0.53$ corresponds to $a = 2$, in which case the $n = 1$ mode should dominate the instability.

excitatory weight and is valid in large regions of parameter space for a Mexican hat. Otherwise the absolute value $|U'(a)|$ must be treated more carefully. Since the input strength $\mathcal{I}$ and pulse width a are related by (3), we eliminate the explicit dependence of $D(a)$ on $\mathcal{I}$ for a Gaussian input by

$$D(a) = \frac{2a}{\sigma^2} I(a) = \frac{2a}{\sigma^2}\big(\kappa(1+\beta) - M(a,a)\big). \tag{10}$$

The pulse width a, determined by $\mathcal{I}$, is a bifurcation parameter of the system, with a Hopf bifurcation occurring at a transverse intersection point of the graphs of $D(a)$ and $D_c^n(a)$ where $D(a) > D_c^n(a)$ fails to hold for all n; see Fig. 2. The spatial extent of the current input σ controls the steepness of $D(a)$ (see (10)), thereby determining which mode destabilizes in the Hopf bifurcation. Importantly, the relative values of $D_c^n(a)$ preserve the ordering of linear dominance of each Fourier mode, indicating which mode should dominate the linear growth. Our analysis thus establishes that a Mexican hat network can undergo a Hopf bifurcation corresponding to excitation of a nonzero Fourier mode ($n > 0$). As we confirm numerically below, this leads to the formation of non radially symmetric breathers. Such behavior should be contrasted with a purely excitatory network, for which the Hopf bifurcation is always associated with excitation of the $n = 0$ mode, thus generating radially symmetric breathers [12]. The latter result follows from equation (9) and the fact that for positive $w(r)$,

$$\begin{aligned}\mu_n(a) &\le 2a\int_0^{\pi} w\big(2a\sin\phi\big)\big|\cos(2n\phi)\big|d\phi\\ &\le 2a\int_0^{\pi} w\big(2a\sin\phi\big)d\phi \equiv \mu_0(a),\end{aligned}$$

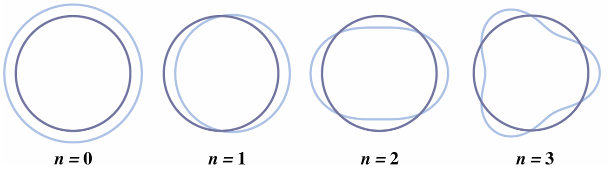

FIG. 3: Small perturbations in terms of Fourier modes (light curves) associated with general perturbations of the threshold boundary of a stationary pulse (dark curves).

The basic structure of the emerging breathers can be predicted by noting that a small perturbation φ of the stationary pulse U results in a small perturbation $\boldsymbol{\delta} = (\delta_r(\theta), \theta)$ of the threshold boundary $\boldsymbol{a} = (a, \theta)$. The corresponding threshold condition is

$$\begin{aligned}\kappa &= u(\boldsymbol{a}+\boldsymbol{\delta}) = U(a+\delta_r(\theta)) + \varphi(\boldsymbol{a}+\boldsymbol{\delta}),\\ &= U(a) + U'(a)\delta_r(\theta) + \varphi(a,\theta) + \mathcal{O}(|\boldsymbol{\delta}|^2).\end{aligned}$$

Using that $U(a) = \kappa$, we find $\delta_r(\theta) = \frac{\varphi(a,\theta)}{|U'(a)|} + \mathcal{O}(|\boldsymbol{\delta}|^2)$. Since φ may be decomposed into Fourier modes in the linear regime, we illustrate in Fig. 3 the perturbative effect of each mode on the threshold boundary. Furthermore, if one mode dominates the linear growth of an instability, we expect the boundary of the breather to develop similar structure. We note that nonradially symmetric instabilities have also been found in a study of homogenous networks, where concentric ring solutions can destabilize into multiple bump solutions, the number of which corresponds to the Fourier mode dominating the instability [14].

Numerical simulations were performed using a Runge-Kutta (RK4) scheme, with a fast-Fourier transform to handle the integral on a rectangular grid and quadrature on an irregular polar grid. The polar grid consists of concentric rings, with each ring increasing the grid point count by one more than the neighboring inner ring. The ring spacing is chosen so that each area element contributes equal weight to the integral. Selecting $\mathcal{I}$ so that the system is positioned beyond the bifurcation point with mode n dominating the instability, the system is evolved from a small random perturbation of the corresponding exact (unstable) stationary pulse solution. Our simulations reveal many types of spatially localized, periodic solutions that are generated by the Mexican hat network. In all cases the periodic solution exhibits a lobed structure, the number of which corresponds to the dominant Fourier mode. Breathers take the general form of emerging and retracting lobes, which often rotate about the input in mirror symmetry, as shown in Fig. 4. On the rectangular grid it is possible to generate breathers for $n = 1, 2, 4, 8$ which exhibit strictly radially expanding/contracting lobes, that do not rotate about the input, as shown in Fig. 5-a. It is likely that such breathers are observed because they are commensurate with the grid.

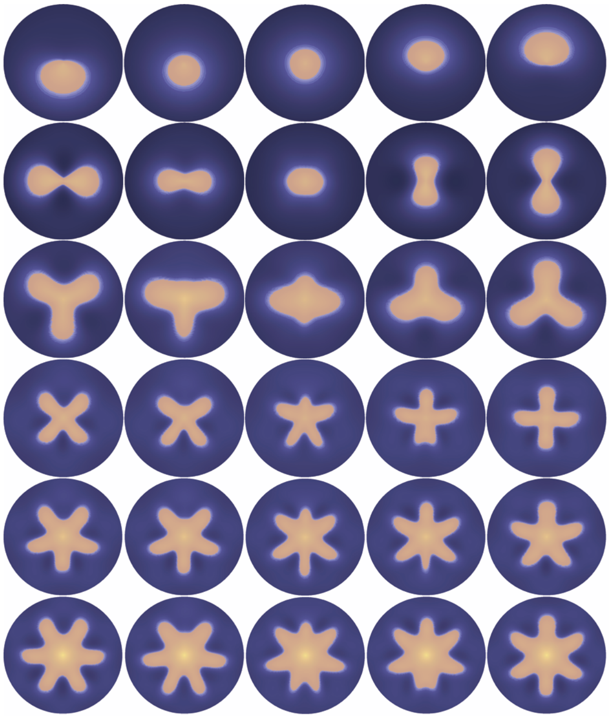

FIG. 4: Breathers for the Mexican hat weight function. Light colors denote suprathreshold values, with the number of lobes corresponding to the dominating unstable Fourier mode.

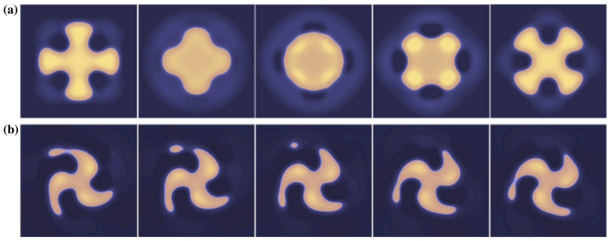

FIG. 5: (a) Strictly expanding/contracting four-fold breather on a rectangular grid. (b) Three-fold rotor.

Interestingly, when the initial transient is sufficiently irregular, or if a sufficiently large initial perturbation with n-fold symmetry is applied, spatially localized rotating solutions (or *rotors*) emerge, see Fig. 5-b.

One of the predictions of our analysis is that breathers may be observed in tangential slices (an effective two-dimensional medium) when a persistent localized input is applied. In the case of disinhibited cortical slices, a radially symmetric input should produce roughly radially symmetric breathers of activity, whereas, if inhibitory connections are maintained, nonradially symmetric breathers should be observed. There are a number of experimental challenges to overcome, however, including the destruction of neurons due to persistent current input and the control of the structure of the input. The use of electric fields by Richardson et al. [2] may be one feasible approach. Experimental verification of breathers may reveal that some form of slow, negative feedback is playing a strong role in the dynamics of neural populations, lending support for the use of rate-based neural network models. Since breathers continue to exist in the presence of inhibition, our work also identifies a mechanism for the generation of stimulus–induced coherent oscillations, which have been suggested to play an important role in the processing of sensory stimuli [15]. From a more general dynamical systems perspective, we have shown how complex spatially localized oscillations can arise in two–dimensional excitable media with nonlocal Mexican hat interactions. This then raises the interesting question as to whether or not analogous dynamical instabilities can occur in diffusively coupled excitable media. Indeed, it has recently been shown that Mexican hat networks exhibit a range of dynamical phenomena also found in three–component reaction-diffusion systems [16].

[1] P. Jung, and J. Milton, Epilepsy as a dynamical disease, Springer (2003).

[2] K. A. Richardson, S. J. Schiff, and B. J. Gluckman, Phys. Rev. Lett. **94**, 028103 (2005).

[3] X. Huang, W. C. Troy, Q Yang, H Ma, C. R. Laing, S. J. Schiff, and J.Y.- Wu, J. Neurosci. **24**, 9897-9902 (2004).

[4] R. Ben-Yishai, R. L. Bar-Or, and H. Sompolinsky, Proc. Natl. Acad. Sci. USA **92**, 3844 (1995).

[5] X. Xie, R. H. R. Haunsloser, and H. S. Seung, Phys. Rev. E **66**, 041902 (2002).

[6] X-J Wang, Trends Neurosci. **24**, 455 (2001).

[7] H. R. Wilson and J. D. Cowan, Kybernetik **13**, 55 (1973).

[8] S. Amari, Biol. Cybern. **27**, 77 (1977).

[9] D. Pinto and G. B. Ermentrout, SIAM J. Appl. Math **62**, 206 (2002).

[10] S. Coombes and M. R. Owen, SIAM J. Appl. Dyn. Syst. **4**, 574-600 (2004).

[11] P. C. Bressloff, S. E. Folias, A. Prat, and Y.-X- Li, Phys. Rev. Lett. **91**, 178101 (2003).

[12] S. E. Folias and P. C. Bressloff , SIAM J. Appl. Dyn. Syst. **3**, 378-407,(2004).

[13] A. Prat, Y-X Li, and P. C. Bressloff, Physica D **202**, 177 (2005).

[14] C. R. Laing, and W. C. Troy, SIAM J. Appl. Dyn. Syst. **2**, 487-516 (2003).

[15] W. Singer, Neuron **24**, 49 (1999).

[16] S. Coombes and M. R. Owen, Phys. Rev. Lett. **94**, 148102 (2005).